ORNL/TM-2021/2189

Report on FY 2021 Testing in Support of Integrating Alloy 800H and 2.25Cr-1Mo for EPP Analysis

Yanli Wang
Peijun Hou
Ting-Leung Sham

September 2021

ORNL/TM-2021/2189

Materials Science and Technology Division

REPORT ON FY 2021 TESTING IN SUPPORT OF INTEGRATING ALLOY 800H AND 2.25CR-1MO FOR EPP ANALYSIS

Yanli Wang
Peijun Hou[1]
Ting-Leung Sham[2]

---

[1] Imtech Corporation, Knoxville
[2] Idaho National Laboratory

September 2021

Prepared by
OAK RIDGE NATIONAL LABORATORY
Oak Ridge, TN 37831-6283
managed by
UT-BATTELLE, LLC
for the
US DEPARTMENT OF ENERGY
under contract DE-AC05-00OR22725

CONTENTS

LIST OF FIGURES

LIST OF TABLES

ABBREVIATIONS

ART	Advanced Reactor Technologies
ASME	American Society of Mechanical Engineers
CC	Code Case
DOE	US Department of Energy
EPP	Elastic-Perfectly Plastic
GCR	Gas-Cooled Reactors (Campaign)
MCR	minimum creep rate
ORNL	Oak Ridge National Laboratory

ACKNOWLEDGMENTS

This research was sponsored by the US Department of Energy (DOE) under contract no. DE-AC05-00OR22725 with Oak Ridge National Laboratory (ORNL), managed and operated by UT-Battelle LLC, and under contract no. DE-AC07-05ID14517 with Idaho National Laboratory, managed and operated by Battelle Energy Alliance. Programmatic direction was provided by the Advanced Reactor Technologies (ART) Program of the Office of Nuclear Reactor Deployment of the Office of Nuclear Energy (NE).

The authors gratefully acknowledge the support provided by Sue Lesica of DOE-NE, Federal Lead, ART Advanced Materials; Diana Li, DOE-NE, Federal Manager, ART Gas-Cooled Reactors (GCR) Campaign; and Gerhard Strydom of Idaho National Laboratory, National Technical Director, ART GCR Campaign.

The authors greatly appreciate ORNL staff members C. Shane Hawkins, Kelsey Hedrick, and Christina Austin for their technical support. The authors wish to thank Edgar Lara-Curzio and Lianshan Lin of ORNL for reviewing this report.

ABSTRACT

The use of simplified Elastic-Perfectly Plastic (EPP) design methods avoids the complexities and limitations of the elastic analysis approach in evaluating strain limits and creep-fatigue damage for Class A metallic coolant boundary components in ASME Boiler and Pressure Vessel Code, Section III, Division 5, Subsection HB, Subpart B. No stress classification and linearization are required in the EPP methods. Further, the strain limits and creep-fatigue damage evaluation procedures based on elastic analysis results were developed for the reactor operating conditions where uncoupled, rate-independent plasticity and stationary creep can be used to approximate the deformation in the component adequately. But at very high temperatures, the deformation is rate-dependent, and it can only be approximated adequately by unified viscoplastic model. Thus, for example, the elastic analysis approach cannot be used to evaluate strain limits and creep-fatigue damage for Alloy 617 above 650 ^{o}C. The EPP methods remove the temperature restriction. They can be used to evaluate strain limits and creep-fatigue damage for the full range of temperatures.

Currently, EPP-based design methods have been qualified for ASME Section III, Division 5 Class A construction using Type 304 and 316 stainless steels, Grade 91 and Alloy 617. Alloy 800H and 2.25Cr-1Mo are the only two remaining Class A materials in ASME Section III, Division 5 that are yet to be integrated into the EPP analysis suite.

This report documents the research and preliminary results in support of the incorporation of Alloy 800H and 2.25Cr-1Mo into the EPP analysis suite. Specialized tests were designed and performed to evaluate the effects of prior cyclic deformation on the subsequent creep properties of these two materials. The results show that prior cyclic loading has an insignificant effect on the minimum creep rate for both materials. Thus, the EPP strain limits and creep-fatigue damage evaluation procedures that have been qualified for Type 304 and 316 stainless steels and Alloy 617 can also be applied to Alloy 800H and 2.25Cr-1Mo. Adjustment factors that were introduced to account for the cyclic softening behavior of Grade 91 are not required for these two materials. Additional tests are recommended to confirm this conclusion.

1. INTRODUCTION

It has been a long-term goal of American Society of Mechanical Engineers (ASME) code committees to develop improved, simplified design rules that are more simply defined, are easier to apply, and take advantage of modern computing capabilities. With recent interests in very high-temperature reactor concepts, there is an added incentive, particularly with the planned use of Alloy 617. The current rules in ASME Section III, Division 5, Subsection HB, Subpart B for the evaluation of strain limits and creep-fatigue damage that use simplified methods based on elastic analysis were deemed inappropriate for Alloy 617 at temperatures above 650 °C. To address these issues, proposed simplified code rules were developed that are based on the use of Elastic-Perfectly Plastic (EPP) analysis methods also applicable at very high temperatures.

The use of simplified EPP analysis methods avoids the complexities and limitations of the traditional ASME linear elastic stress classification design methods. The simplified methods exploit the fact that EPP methods naturally handle the stress redistribution, which is the key to stress classification schemes. For high-temperature design, creep strain and stress redistribution occur naturally during service. The EPP methods use pseudo-yield stress to account for stress and strain redistribution, and the definition of pseudo-yield stress requires the consideration of creep effects at elevated temperature.

Currently, EPP-based design methods have been qualified for ASME Section III, Division 5, Class A applications for Alloy 617 via Code Case (CC) N-898, as well as for Type 304 and 316 stainless steel via two approved CCs: strain limits (CC N-861) and EPP creep fatigue (CC N-862). All three materials exhibit cyclic hardening behavior. Thus, the pseudo yield stress based on the isochronous stress-strain curves conservatively lower bounds the stresses in the component under cyclic loading.

Unlike Type 304 and SS316 stainless steel and Alloy 617, Grade 91 is a strong cyclic softening material. EPP analysis based on monotonic material properties can potentially result in a lack of conservatism (Messner and Sham 2017, 2018, 2019). Experimental and modeling research was carried out to support the extension of the EPP Code Cases to Grade 91 for design analysis (Messner and Sham 2017, 2018, 2019; Wang et al, 2017, 2019). Temperature and time dependent reduction factors were developed and applied to the isochronous stress-strain curves obtained without prior cyclic deformation to account for the cyclic softening effect (Messner and Sham, 2019), and a specially designed experiment was performed to verify these reduction factors (Wang et al, 2017, 2019). The EPP strain limits Code Case was revised to incorporate Grade 91 by introducing the reduction factors in CC N-861. The revision, CC N-861-1, was approved in 2019.

Alloy 800H and 2.25Cr-1Mo are the two remaining Class A materials in ASME Section III, Division 5 that are yet to be integrated to EPP analysis suite. Verification and justification are required to allow the use of the simplified EPP methods for the design of reactor components constructed with these two Class A materials. Recent interests for advanced reactor development placed the task of extending EPP analysis to these two materials at a higher priority. As part of the research effort in support of the incorporation of Alloy 800H and 2.25Cr-1Mo in the EPP analysis suite, experiments were initiated using a specialized testing approach to evaluate the effects of prior cyclic deformation on the creep properties of Alloy 800H and 2.25Cr-1Mo. The goal of this research is to verify whether the EPP design rules for Type 304 and 316 stainless steels and Alloy 617 are applicable to Alloy 800H and 2.25Cr-1Mo, or reduction factors similar to those introduced for Grade 91 are required for these two materials. The results from these experiments are summarized in this report.

2. MATERIALS

2.1 ALLOY 800H

Alloy 800H is an approved Class A material in the ASME code for nuclear applications up to 760°C with a maximum design life of 300,000 h. The Alloy 800H material with a heat number of 37458 used in this study was a historical reference plate material stored at ORNL. The plate was manufactured by Jessop Steel Company in 1989 and has a factory marking of UNS 08811, which indicates that it meets ASTM B409-87 specification, an earlier version of ASTM B409-06 specification. The chemical compositions of the Alloy 800H are listed in Table 1, which also confirms that it meets ASTM B409-06 requirements. The total of Al plus Ti content is 0.88 wt % and meets the minimum requirements of 0.50 wt % per ASME Section III, Division 5 Table HBB-I-14.1(a). Additionally, Wright et al. (2010) performed a very detailed characterization of Alloy 800H material and reported that this heat meets the Alloy 800H specifications such as grain size and tensile properties.

Table 1. Chemical compositions of Alloy 800H (heat number 37458) compared with the chemical requirements of ASTM B409-06 (wt %).

Alloy 800H	Ni	Cr	Fe	Mn	C	Cu	Si	S	Al	Ti	Mo	Co
Heat no. 37458	30.45	19.30	47.05	1.31	0.063	0.21	0.37	0.001	0.43	0.45	0.21	0.11
ASTM 409B-06	30.0–35.0	19.0–23.0	39.5 min.	1.5 max.	0.06–0.10	0.75 max.	1.0 max.	0.015 max.	0.15–0.6	0.15–0.6	-	-

2.2 2.25CR-1MO

A forging grade 2.25Cr-1Mo bar material manufactured by TimkenSteel with heat number of J6613 was purchased in support of this research. The as-received 2.25Cr-1Mo bars meet ASTM A182 chemistry requirements, as listed in Table 2. The as-received bar material with a nominal diameter of 1.250 in was hot-rolled, normalized, and tempered. This manufacturing process produces material properties within the category of Grade F22 Class 3. However, ASME Section III, Division 5 Table HBB-I-14.1(a) requires the forging grade to be Class 1; thus, an additional heat treatment was performed at ORNL to return the material to the required annealed condition. The heat treatment was performed at 954.4℃ (1750 °F) for 2 h followed by furnace cool in air.

Table 2. Chemical compositions of 2.25Cr-1Mo (heat number J6613) compared with the chemical requirements of ASTM A182 (wt %).

2.25Cr-1Mo	C	Cr	Mn	Cu	Si	S	Al	P	Mo	Ni	Fe
Heat No. J6613	0.13	2.45	0.58	0.20	0.32	0.016	0.026	0.010	1.03	0.13	47.05 bal.
ASTM A182	0.05–0.15	2.0–2.5	0.30–0.60	-	0.50 max.	0.025 max.	-	0.025 max.	0.90–1.10	-	-

Room-temperature tensile tests were performed on specimens under the annealed condition, following ASTM E8. The tensile results are presented in Figure 1 and Table 3. ASME Section III, Division 5 Table HBB-I-14.1(a) requirements of a minimum specified room-temperature yield strength of 207 MPa, a minimum specified room-temperature ultimate strength of 414 MPa, and a maximum specified room-temperature ultimate strength of 586 MPa are satisfied.

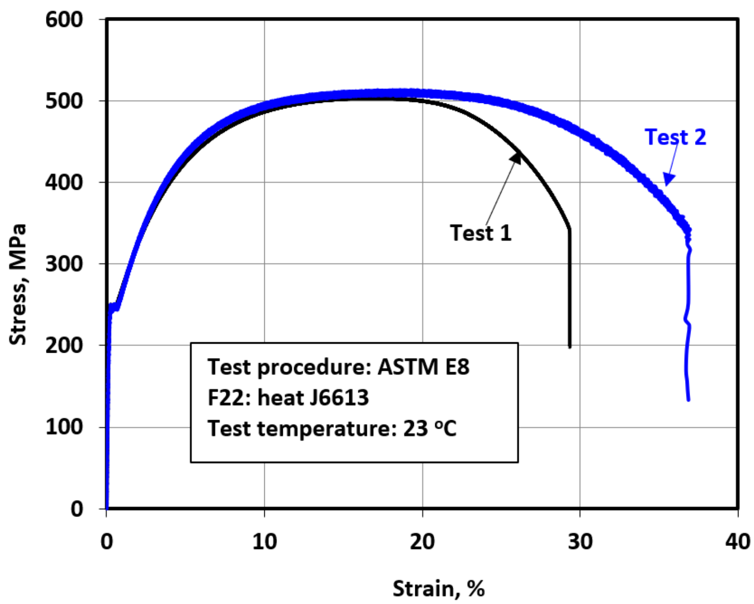

Figure 1. Room-temperature tensile tests on 2.25Cr-1Mo (heat number J6613).

Table 3. Room-temperature tensile test results on 2.25Cr-1Mo (heat number J6613).

	Yield strength (MPa)	**Ultimate tensile strength (MPa)**	**Total elongation (%)**	**Uniform elongation (%)**	**Reduction of area, %**
Test 1	243.6	503.3	29.3	16.6	62.7
Test 2	244.6	510.2	33.7	19.5	62.2

Typical microstructure images observed under a scanning electron microscope (SEM) are presented in Figure 2 at both high and low magnifications, showing a typical ferritic-bainitic microstructure. The microstructure was uniform across the diameter.

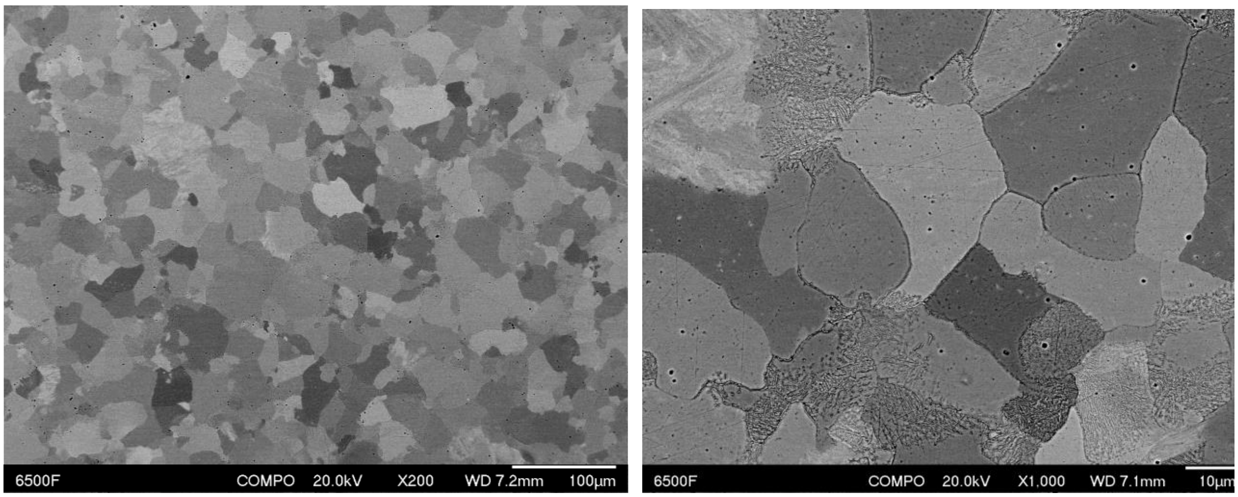

(a) (b)

Figure 2. SEM images of 2.25Cr-1Mo (heat number J6613) at (a) low and (b) high magnifications.

Additionally, Vickers hardness measurements with 300 g of force were performed along two inspection lines 5 mm apart on the cross section of the 2.25Cr-1Mo bar. The locations of the Vickers hardness measurements and the results are presented in Figure 3. The average Vickers hardness value is 145 and is uniform across the diameter.

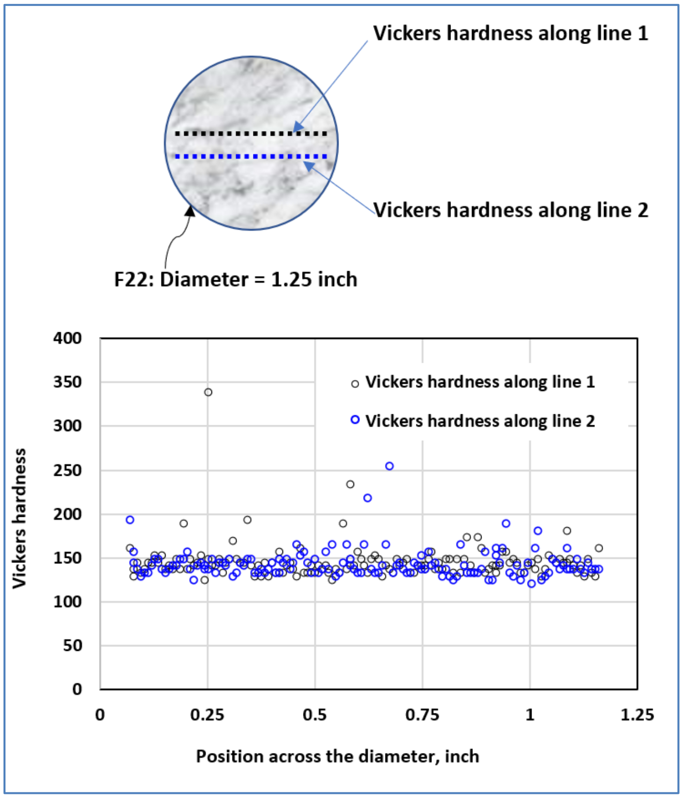

Figure 3. Vickers hardness measurement locations and the results on 2.25Cr-1Mo (heat number J6613).

3. EXPERIMENTAL APPROACH

Elastic-Perfectly Plastic (EPP) analysis procedures for cyclic hardening materials and cyclic softening materials were developed in ASME Section III, Division 5 through two Division 5 Code Cases. These EPP-based design methods have been qualified for applications for Type 304 and 316 stainless steels, Alloy 617, and Grade 91. These approved materials for the EPP analysis suite are categorized as either cyclic hardening (Type 304 and 316 stainless steels and Alloy 617) or cyclic softening (Grade 91). The evaluation method used in determining the effect of cyclic softening on the creep behavior of Grade 91 for EPP analysis was documented in Wang et al. (2017, 2019) and Messner and Sham (2019). The same evaluation procedure was adopted in this study, and the effect of prior cyclic deformation on creep properties is evaluated by introducing strain-controlled cyclic fatigue segments into a creep test. The changes in the minimum creep rate (MCR) due to prior fatigue cycles are used to determine whether reduction factors are required to modify the isochronous stress-strain curves to account for any cyclic softening effects (Messner and Sham 2017).

Figure 4 schematically illustrates the testing protocol implemented in a servo-hydraulic machine. The test starts with a load-controlled creep segment followed by unloading to zero load before switching the test machine to the strain-controlled mode and cycling for a specified number of fatigue cycles. The creep and fatigue segments are repeatedly applied to the same specimen until failure occurs.

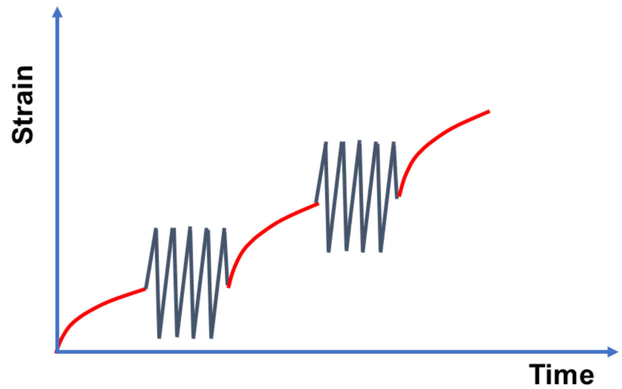

Figure 4. Schematics of the sequential creep and fatigue experiments.

To seamlessly switch between the creep segment under the load-controlled mode and the fatigue segment under the strain-controlled mode, the mode-switching function of the servo-hydraulic machine was exploited. The suitable test specimen for this evaluation is the standard creep-fatigue specimen geometry shown in Figure 5.

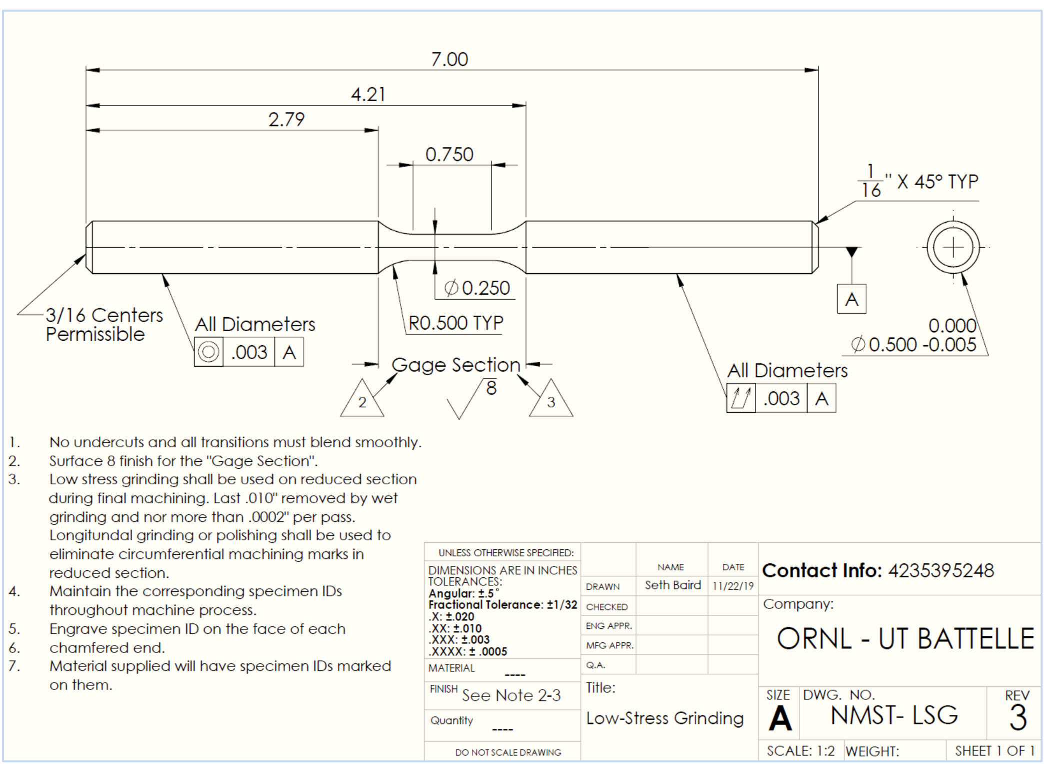

Figure 5. Standard creep-fatigue specimen geometry. Dimensions are in inches.

Table 4 lists the detailed testing parameters. Alloy 800H was tested at 750 °C, and 2.25Cr-1Mo was tested at 650 °C. These temperatures are high enough to ensure that the tests were in the creep region. The stress levels for the creep segment were selected to result in relatively shorter creep rupture times (i.e., several thousand hours). The strain-controlled fatigue segments were fully reversed with a triangle shape waveform. A strain range of 0.8% was selected to allow at least five fatigue segments be applied before failure initiation. The strain-controlled fatigue testing procedures are consistent with ASTM E606.

Table 4. Test parameters for sequential creep and fatigue on Alloy 800H and 2.25Cr-1Mo.

Material		**Alloy 800H**	**2.25Cr-1Mo**
Test temperature		750 °C	650 °C
Load-controlled creep segment	Applied stress	55 MPa	42 MPa
	Loading rate	0.5 s to the stress level	0.5 s to the stress level
Strain-controlled fatigue segment	Strain range	0.8%	0.8%
	Strain rate	1E-3/s	1E-3/s
	Loading ratio, *R*	-1	-1
	Number of cycles applied in each fatigue segment	150	200

In parallel, baseline creep tests are also being performed on standard creep frames at the same stress levels, i.e., 55 MPa at 750 °C for Alloy 800H and 42 MPa at 650 °C for 2.25Cr-1Mo. The testing procedure follows ASTM E139. The creep specimen has the same nominal diameter of 0.250 in, and the geometry is shown in Figure 6. These standard uninterrupted creep tests are used to evaluate the creep behavior of these two materials under the same stress levels at the same test temperature. These standard creep tests can provide baseline information in determining the effect of the addition of prior fatigue cycles on their creep behavior, and to check if the creep properties of these two materials used in this study are representative of the materials used to generate the database for developing the rupture stresses in the ASME Code.

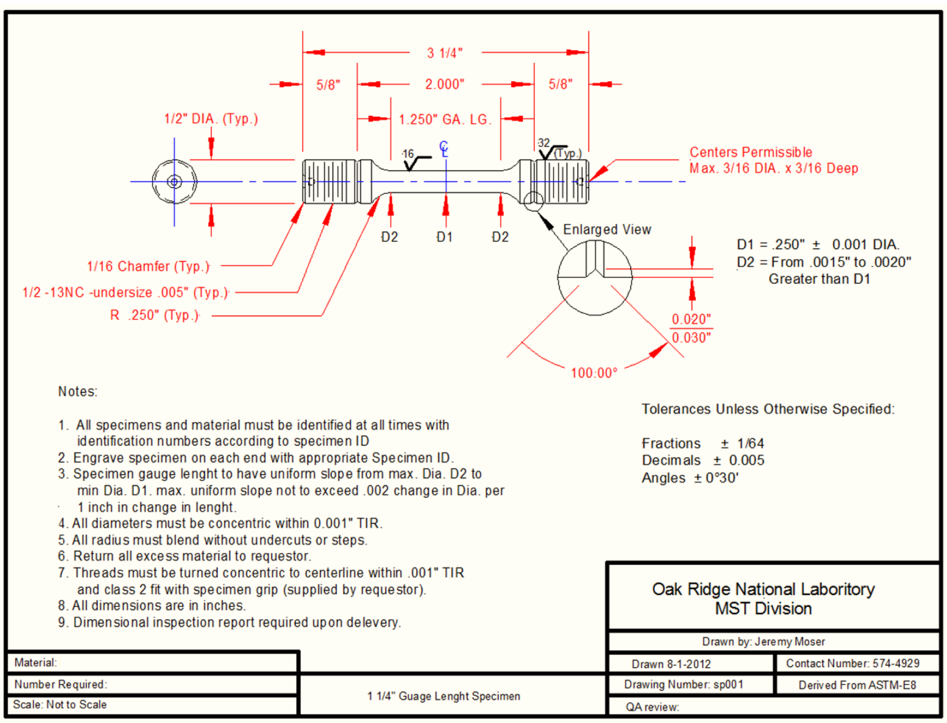

Figure 6. Standard creep specimen geometry. Dimensions are in inches.

4. EFFECTS OF CYCLIC LOADING HISTORY ON CREEP PROPERTIES

4.1 PRELIMINARY RESULTS ON ALLLOY 800H

The experiment on Alloy 800H with combined sequential creep and fatigue at 750 °C was tested to failure. Seven fatigue segments with 150 cycles each at a 0.8% strain range were performed, and five fatigue segments were applied before fatigue failure initiation at the beginning of segment 6. The maximum and minimum stresses of all the fatigue segments are presented in Figure 7, in which the segment numbers are labeled on the maximum stress plot. The fatigue segments showed cyclic hardening at the initial ~10 cycles and then it stabilized at the peak stress thereafter.

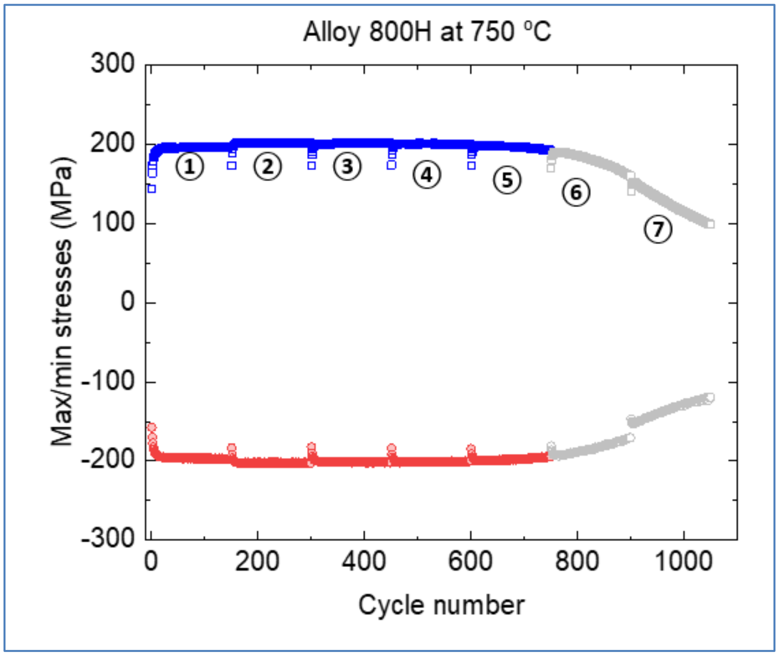

Figure 7. Maximum and minimum stresses of the fatigue segments on Alloy 800H at 750 °C.

Prior to each fatigue segments, there was a creep segment with an applied stress of 55 MPa. The creep curves of all the creep segments are plotted in Figure 8. Because segments 6 and 7 were collected the initiation of fatigue failure, the creep curves from these two segments are for information only and were not used for the evaluation of the effect of the prior cyclic deformation on creep properties. The creep times of the first two segments were longer to get into the steady-state creep regime as closely as possible. Table 5 summarizes the test duration, the accumulated creep strain at the end of the segment, and the MCR for the first five creep segments. The total accumulated creep time from these segments was 184.6 h, and the total accumulated creep strain was 0.437%.

The baseline uninterrupted standard creep test for Alloy 800H at 55 MPa and 750 °C is still running at the time of writing this report. The available creep data from this test were collected and are plotted in Figure 9. This test showed a short steady-state creep region of less than 400 h and then it started to exhibit increasing creep rates. The MCR was 4.05e-4%/h, calculated from the short steady state stage of the creep curve, indicated by the red dotted line on the plot. The total creep strain was 0.29% at a creep time of 184.6 h, which is much less than the test with alternating creep segment and fatigue segment.

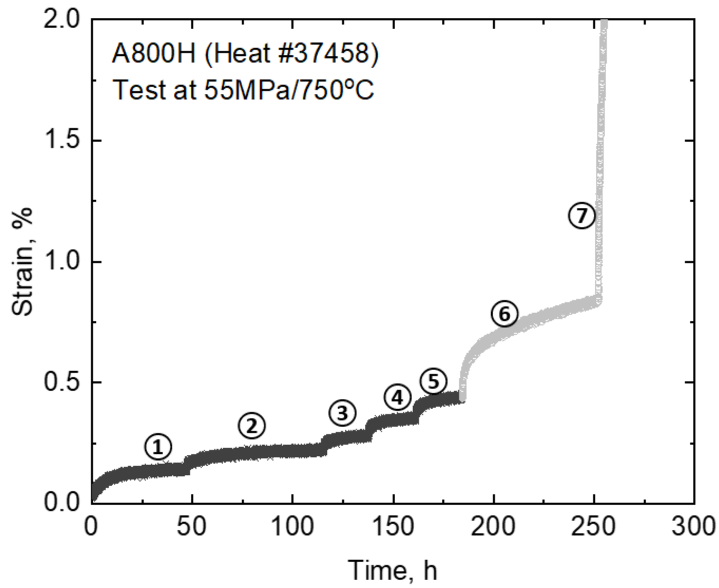

Figure 8. Creep curves from the creep segments on Alloy 800H under 55 MPa at 750 °C.

Table 5. Summary of the creep segments on Alloy 800H at 55 MPa and 750 °C.

Segment no.	Prior fatigue cycles (% of fatigue damage)	Duration (h)	Accumulated creep strain (%)	MCR (%/h)
Creep 1	0/0	47.3	0.132	5.27E-04
Creep 2	150 (20%)	68.1	0.222	3.32E-04
Creep 3	300 (40%)	22.2	0.282	6.11E-04
Creep 4	450 (60%)	23.5	0.362	6.88E-04
Creep 5	600 (80%)	23.2	0.437	8.60E-04

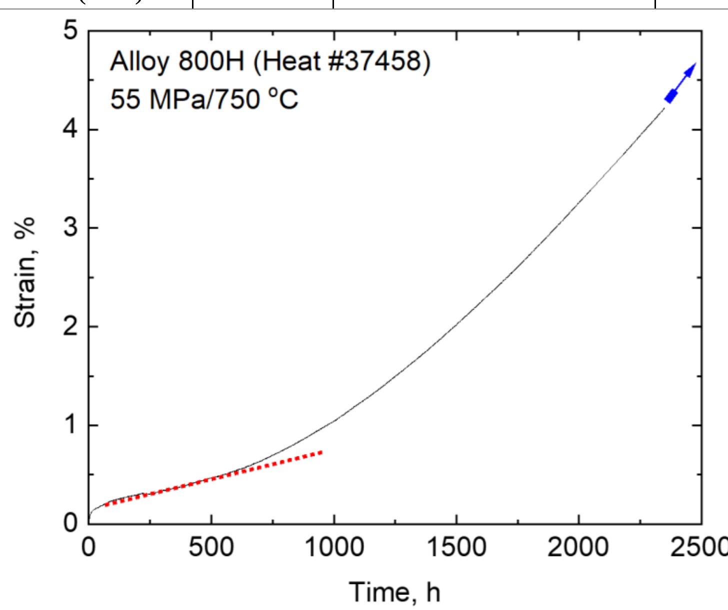

Figure 9. Creep curve of the standarnd uninterupted test on Alloy 800H under 55 MPa at 750 °C.

It is evident for the test with alternating creep segment and fatigue segment, the re-starting process of each creep segment has resulted in a renewed primary creep stage and more creep strain was accumulated since the primary creep stage has higher creep rates than the MCR. It is not surprising that the test with alternating creep segment and fatigue segment accumulated higher total creep stain than the standard uninterrupted creep test.

4.2 PRELIMINARY RESULTS ON 2.25CR-1MO

This section summarizes the test on 2.25Cr-1Mo with alternating creep segment and fatigue segment at 650 °C. Six fatigue segments with 200 cycles per segment at 0.8% strain range were performed, and five full fatigue segments were completed prior to the fatigue failure initiation. The maximum and minimum stresses of all the fatigue segments are presented in Figure 10, which the segment numbers are labeled on the maximum stress plot. Similar to Alloy 800H, the results show initial cyclic hardening for the first few cycles and then it stabilized at the peak stress thereafter.

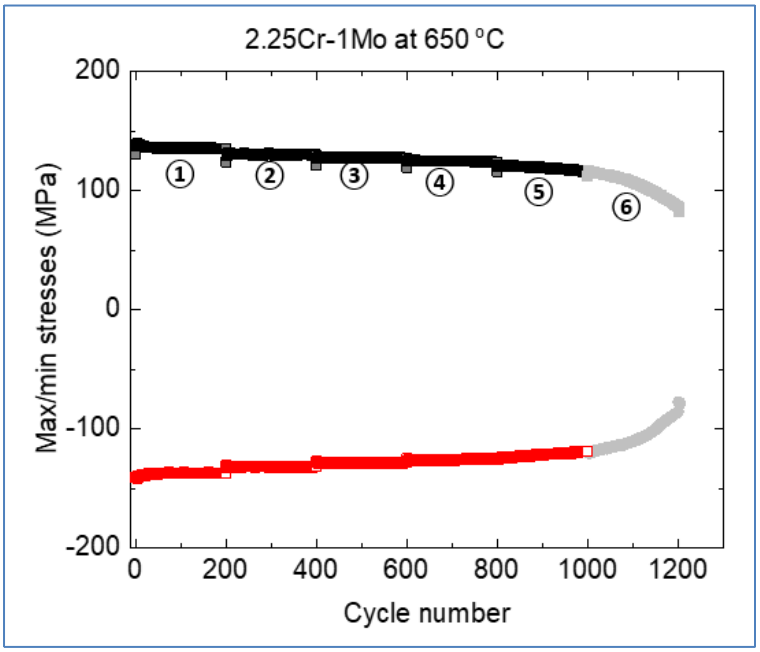

Figure 10. Maximum and minimum stresses of the fatigue segments on 2.25Cr-1Mo at 650 °C.

The applied stress for each of the creep segment was 42 MPa. The creep curves of all the creep segments are plotted in Figure 11. Because segments 6 and 7 were collected after the fatigue failure initiation, the creep curves from these two segments were not used for evaluation of the effect of prior cyclic deformation on the creep properties. The creep duration time of the first segment was 70.4 h, longer than those of the remaining segments. The longer creep time ensured that the test reached the steady-state creep stage. Table 6 summarizes the test duration, the accumulated creep strain at the end of the segment, and MCR for the first five creep segments. The accumulated creep time was 231.85 h from these five segments, and the accumulated creep strain was 0.925%.

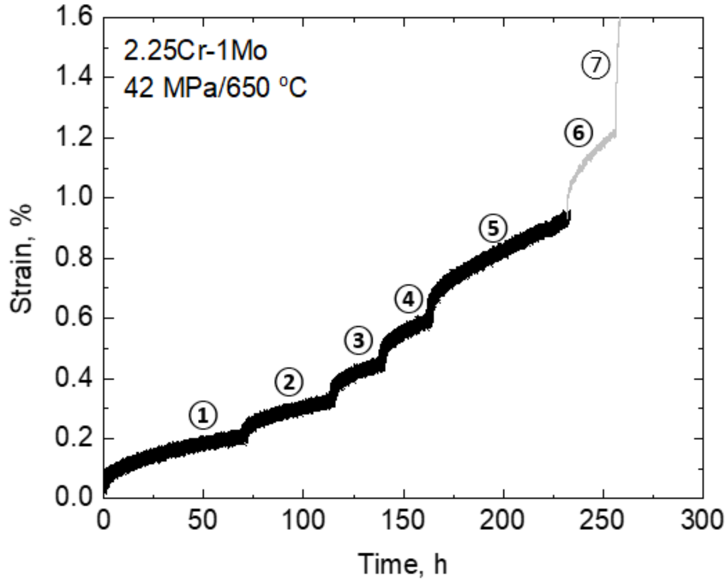

Figure 11. Creep curves from the creep segments on 2.25Cr-1Mo under 42 MPa at 650 °C.

Table 6. Summary of the creep segments on 2.25Cr-1Mo at 42 MPa at 650 °C.

Segment no.	Prior fatigue cycles (% of fatigue damage)	Duration (h)	Accumulated creep strain (%)	MCR (%/h)
Creep 1	0(0)	70.4	0.208	1.13E-03
Creep 2	200 (20%)	44.3	0.308	1.67E-03
Creep 3	400 (40%)	24.7	0.460	2.10E-03
Creep 4	600 (60%)	23.8	0.582	3.13E-03
Creep 5	800 (80%)	68.6	0.925	2.73E-03

The baseline uninterrupted standard creep test is still running at 650°C at the time of writing this report. The available creep data from this test were collected and are plotted in Figure 12. This test entered the steady-state creep stage after approximately 35 h. The test had not yet entered the tertiary creep stage at the time of writing this report. The MCR was 3.69e-3%/h, and the total creep strain was 1.10% at a creep time of 231.85 h.

It is noted that the standard creep test has higher MCR than those from the test with alternate creep segments and fatigue segments. Although the actual stress level applied to this test was slightly higher at 44.2 MPa, the difference in the MCR between these two tests could possibly due to specimen-to-specimen variation.

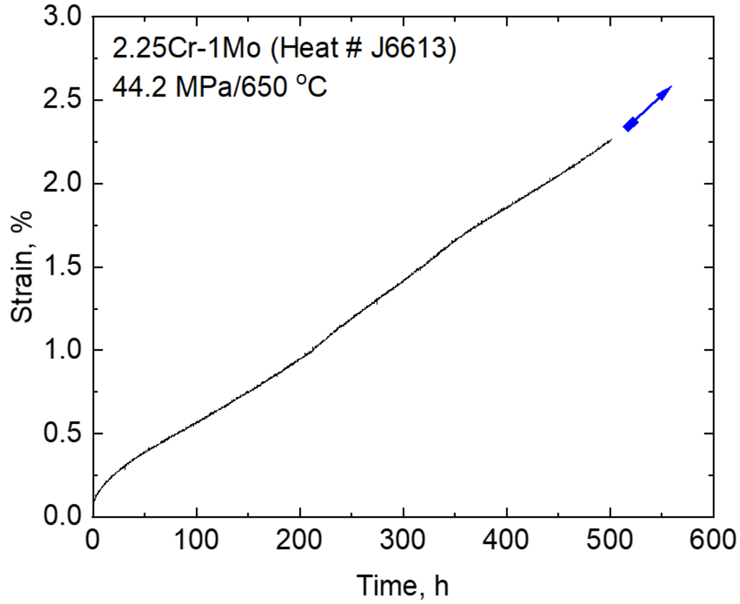

Figure 12. Creep curve of the standard uninterrupted test on 2.25Cr-1Mo under 44.2 MPa at 650 °C.

4.3 DISCUSSIONS

The reduction factors to account for the cyclic softening effect on isochronous stress-strain curves were determined from the changes in the MCR due to prior cyclic deformation (Messner and Sham 2019). These changes in the MCR are presented by normalizing the MCR measured from each segment with that from the first segment. Because the first segment did not have any prior cyclic deformation, it represents the behavior of a standard creep test. The normalized MCRs of the creep segments for Alloy 800H at 750 ℃/55 MPa and 2.25Cr-1Mo at 650 ℃/42 MPa are plotted in Figure 13. For comparison, the results for Grade 91 at three test conditions— 600 ℃/150 MPa, 625 ℃/130 MPa, and 650 ℃/99 MPa—are also presented in the same figure to demonstrate the strong cyclic softening effect on the MCRs for Grade 91 (Wang et al. 2019).

With 80% of the fatigue damage, the Grade 91 specimens were either ruptured or experienced an increased MCR of more than 30 times higher than the MCR without prior cyclic deformation, illustrating the significant cyclic softening effect on Grade 91. In contrast, Alloy 800H and 2.25Cr-1Mo both showed an increase of less than three times in the MCR when comparing the MCR at 80% fatigue damage to that of the first creep segment. With the uncertainties in the measurements—such as noises in the strain signals, variations of the testing temperature during the test, and specimen-to-specimen variation—the changes in the MCR for these two tests are deemed to be insignificant. Thus, it is not recommended to incorporate any softening factor for Alloy 800H and 2.25Cr-1Mo when they are incorporated to the EPP analysis suite, although additional testing on these two materials is desired to confirm this recommendation.

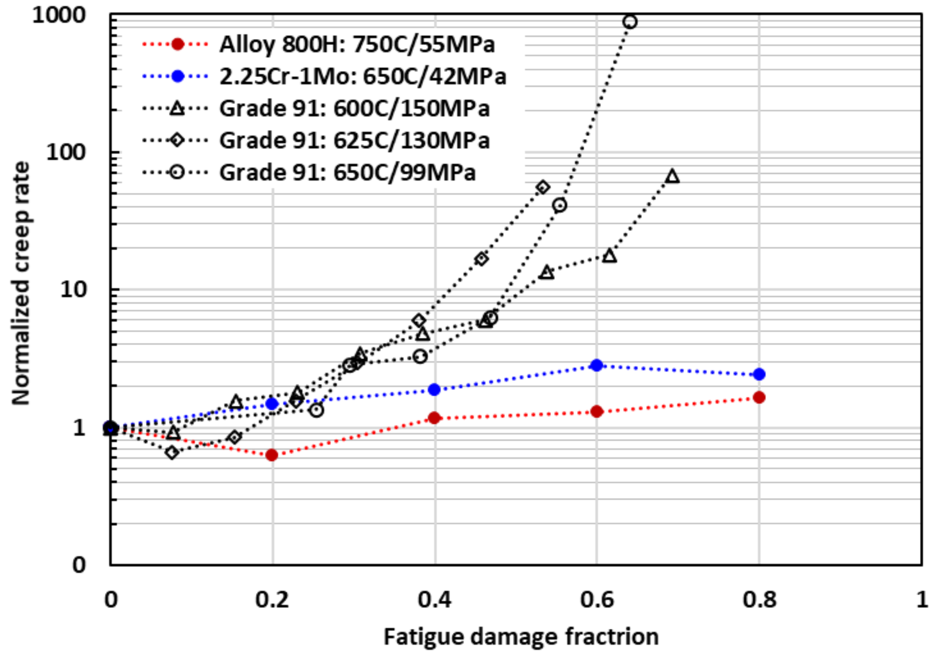

Figure 13. Effect of fatigue cycling history on the MCRs of Alloy 800H, 2.25Cr-1Mo, and Grade 91.

5. SUMMARY

Experiments were designed and performed on Alloy 800H and 2.25Cr-1Mo in support of the extension of ASME EPP analysis suite to these two Class A materials in ASME Section III Division 5. The results show that prior cyclic deformation has an insignificant effect on the MCR for both materials; therefore, reduction factors on the isochronous stress-strain curves are not recommended when incorporating Alloy 800H and 2.25Cr-1Mo to the EPP analysis suite. Additional tests are recommended to confirm this assessment.

6. REFERENCES

ASME. 2019a. Boiler and Pressure Vessel Code, Section III Division 5, *Rules for Construction of Nuclear Facility Components*, Subsection HB Subpart B, American Society of Mechanical Engineers, New York, NY (2021 Edition).

ASME B&PV Code Case N-861, *Satisfaction of Strain Limits for Division 5 Class A Components at Elevated Temperature Service Using Elastic-Perfectly Plastic Analysis*, ASME Section III Division 5.

ASME B&PV Code Case N-862, *Calculation of Creep-Fatigue for Division 5 Class A Components at Elevated Temperature Service Using Elastic-Perfectly Plastic Analysis Section III, Division 5,* ASME Section III Division 5.

ASME B&PV Code Case N-898, *Use of Alloy 617 (UNS N06617) for Class A Elevated Temperature Service Construction*, ASME Section III Division 5.

ASTM A182 / A182M-21, *Standard Specification for Forged or Rolled Alloy and Stainless Steel Pipe Flanges, Forged Fittings, and Valves and Parts for High-Temperature Service*, ASTM International, West Conshohocken, PA, 2021, www.astm.org

ASTM B409-06(2016), *Standard Specification for Nickel-Iron-Chromium Alloy Plate, Sheet, and Strip*, ASTM International, West Conshohocken, PA, 2016, www.astm.org

ASTM E8 / E8M-21, *Standard Test Methods for Tension Testing of Metallic Materials*, ASTM International, West Conshohocken, PA, 2021, www.astm.org

ASTM E139-11, *Standard Test Methods for Conducting Creep, Creep-Rupture, and Stress-Rupture Tests of Metallic Materials*, ASTM International, West Conshohocken, PA, 2011, www.astm.org

ASTM E606 / E606M-21, *Standard Test Method for Strain-Controlled Fatigue Testing*, ASTM International, West Conshohocken, PA, 2021, www.astm.org

Messner, M. C. and Sham, T.-L., (2017), *FY17 Status Report on the Initial EPP Finite Element Analysis of Grade 91 Steel*, Technical Report No. ANL-ART-94, Argonne National Laboratory, Chicago, IL.

Messner, M. C. and Sham, T.-L. (2018), *Initial development and extension of EPP methods to Grade 91*, ANL-ART-133, Argonne National Laboratory, Chicago, IL.

Messner, M. C. and Sham, T.-L. (2019), *Draft ASME Section III Division 5 Code Cases to extend EPP strain limits and creep-fatigue design methods to Grade 91*, ANL-ART-165, Argonne National Laboratory, Chicago, IL.

Wang, Y., M. C. Messner, and T.-L. Sham. 2017. *FY17 Status Report on Testing Supporting the Inclusion of Grade 91 Steel as an Acceptable Material for Application of the EPP Methodology*, ORNL/TM-2017/388. Oak Ridge, TN: Oak Ridge National Laboratory.

Wang, Y., Jetter, R. I., Messner, M. C. and Sham, T.-L. (2019), *Report on FY19 Testing in Support of Grade 91 Core Block Code Case*, ORNL/TM-2019/1280, Oak Ridge National Laboratory, Oak Ridge, TN.

Wright, J. K., Wright, R. N., and Sham T.-L., (2010), *Next Generation Nuclear Plant Steam Generator and Intermediate Heat Exchanger Materials Research and Development Plan*, INL/EXT-08-14107 Rev. 1, Idaho National Laboratory, Idaho Falls, ID.